Leadership in Sustainable Infrastructure
Leadership en Infrastructures Durables

Vancouver, Canada
May 31 – June 3, 2017/ *Mai 31 – Juin 3, 2017*

EXPERIMENTAL AND NUMERICAL MODELING OF HYDRODYNAMIC LOADING ON PIPELINES DUE TO EXTREME HYDRODYNAMIC CONDITIONS

Ghodoosipour, Behnaz[1,4], Nistor, Ioan[3] and Mohammadian, Abdolmajid[3]
[1] PhD student, University of Ottawa, Canada,
[2] Professor, University of Ottawa, Canada
[3] Associate professor, University of Ottawa, Canada
[4] bghod068@uottawa.ca

Abstract

Pipelines in coastal areas are used for gas and oil transportation, as well as for disposal of wastewater to water bodies. Installation of pipelines in coastal areas is of great importance, and requires consideration of different engineering design criteria. A new topic in pipeline design has emerged lately due to the recent extreme hydrodynamic events such as tsunami and storm surges. Therefore, the primary objective of this study was to investigate the hydrodynamic forces induced on pipelines during such extreme waves. A comprehensive program of physical model experiments were conducted in the Hydraulic Flume at the University of Ottawa. The tests attempted to measure the hydrodynamic forces exerted on pipe due to tsunami-like bores replicated using dam break flow. Different pipe placement configurations using different gap ratios (e/D), (e being distance to bottom and D pipe's Diameter), were tested under various flow conditions in wet and dry bed. For the case of dry bed conditions, experimental results show that only for e/D ≤ 0.3, two peaks are noticeable in force time-history, whereas, for other relative gap ratios, no distinct peak was noticed. The main reason for such behavior when using small e/D ratios is the suppression of the vortex shedding which forms around the pipe. For the case of wet bed conditions, the time-history of the drag force shows no change even when drastically changing the relative gap ratio. The 1-D shallow water equations were also used to study the dam break flow over the flat flume bed and its impact with the circular cylinder downstream of the flow. The drag coefficient was then derived using experimental and numerical results and showed relatively good agreement between the two. Results from this study will be used for the assessment of the current design recommendations with the ultimate goal of improving them.

1. Introduction

The design of pipelines to withstand external loading exerted on them requires a proper understanding of the external hydrodynamic forces. Existing literature on this important subject goes back to Morison et al. [1950], who proposed a widely-accepted formulation of the forces on water surface-piercing piles due to ocean waves. Morison equation could be applied to derive the forces exerted on the center of a pipe as:

$$[1.1] \quad F = \underbrace{\rho C_m V \dot{u}}_{F_I} + \underbrace{\frac{1}{2}\rho C_d A u|u|}_{F_D}$$

where F_I is inertia force due to the accelerating flow, C_m is the inertia (mass) coefficient, $\dot{u}$ is the flow acceleration, V is the volume of the pipe, F_D is the drag force caused by fluid viscosity and the velocity gradient within the thin boundary layer next to the cylinder's surface, C_d is the drag coefficient, *A* is the area

of the pipe projection perpendicular to the direction of the flow and *u* is the horizontal flow velocity. Variations of the above formula to calculate the hydrodynamic forces in steady and oscillatory flows exerted on horizontal cylinders were reported in other articles. Flow around circular cylinders is complex: vortex shedding suppression occurs at Reynolds numbers above critical values, subsequently changing the pressure distribution around the cylinder and causing extra fluctuations of the drag and lift forces to act on the cylinder (Lei et al [1999]). Drag and lift coefficients are non-dimensional and dependent on both the flow and the cylinder geometry and location. For cylinders placed near the bottom boundary, bed roughness, turbulent behaviour and velocity gradient of the boundary layer play an important role on the force exerted on the cylinder. Several experimental studies focused on issues related to cylinders located near a plane boundary. Most studies revealed a critical distance to bottom ratio (e/D=0.3) defined as the distance for which vortex shedding suppression occurs. Bearman et al. [1978], Angrilli et al. [1982] and Zdravkovich, [1985] proposed this hypothesis by looking into the power spectra of hot wire signals occurring in the wake region of a cylinder. However, Buresti & Lanciotti's [1992] results show e/D=0.4 to be the critical relative gap ratio. The existence of vortex shedding causes the occurrence of a peak in the power spectra which disappears due to the vortex shedding suppression in a specific gap ratio called vortex shedding suppression gap ratio.

In recent years, a new criteria has emerged in pipeline design due to the recent catastrophic events such as tsunamis and storm surges which caused massive damaging consequences of such infrastructure. The 2011 Tohoku Tsunami in Japan and the 2012 Typhoon Haiyan in the Philippines, raised an increased interest of research groups to re-evaluate the existing design and safety codes such that they would consider effects of such extreme events. The American Society of Civil Engineers (ASCE), through its ASCE7 Tsunami Loads and Effects Subcommittee, has developed a new standard for tsunami impacts and loading (Chock [2016]) and has emphasized the need to investigate tsunami loads on pipelines located in tsunami-prone areas.

Different studies have focused on investigating forces induced by a hydraulic bore on infrastructure: among them Stoker [1957], and Cross [1967]. Stoker [1957] have used nonlinear shallow water equations to study the behaviour of bores for a moving hydraulic jump surging over still water layer. Guidelines for the Design of Structures for Vertical Evacuation from Tsunamis FEMA P-646 [2012] introduces forces exerted on a body during a tsunami as drag and impulse force. The lateral component of hydrodynamic force is called drag force and is a combination of the pressure force and the friction force due to the fluid. The drag force can be calculated using

$$[1.2] \quad F_d = \frac{1}{2}\rho_s C_d B(hu_{max}^2)$$

Where ρ_s is the fluid density, *Cd* is the drag coefficient, *B* is the width of the structure in the plane normal to the direction of flow, *h* is flow depth, and *u* is the flow velocity at the location of the structure. For forces on structural components, *B* is taken as the width of the component. The drag coefficient depends mainly on structure geometry. hu_{max}^2 is the maximum momentum flux per unit volume where u_{max} is the maximum velocity during tsunami and *h* is the corresponding water depth at the instant when velocity is maximum.

The impulse force is caused by bore front impacting the structure. Experiments conducted on measuring impact force show that in dry bed conditions, there is no considerable peak in the force time-history at the time of impact. However, experimental work recorded a considerable force peak in wet bed condition (Ramsden [1993]). Arnason [2005], estimated the maximum impact force to be approximately 1.5 times larger than the corresponding drag force.

Due to the need for increased protection of pipelines against extreme hydrodynamic events, the main objective of this study is to investigate the induced hydrodynamic forces on pipelines during extreme waves and flood events. The drag coefficient plays an important role in the magnitude of the drag force. Suggested values in existing guidelines for drag coefficient are mostly derived for steady or oscillatory flows. Because of the unsteady behavior of tsunami-induced inland inundation, the drag coefficient changes with time in

contrast to the case of steady flow conditions in which the drag coefficient is constant (Arnason [2005]). This study proposes values for drag coefficient in the case of a transient dam break flow for different relative gap ratios.

2. Experimental Methodology

The objective of this experimental study was to characterise hydrodynamic forces exerted on pipelines due to extreme events, modelled using dam break waves. A comprehensive experimental approach was conducted for this purpose. Different parameters were varied during the experiments namely, reservoir depth (h), tailewater depth (d), pipe distance to bottom (e) to diameter (D) ratio (e/D). More than 500 tests were conducted at the hydraulic flume in university of Ottawa.

2.1. Experimental setup

2.1.1. Flume and impoundment reservoir

The experiments were conducted in the Hydraulic Flume in the Hydraulic Laboratory at the Department of Civil Engineering at the University of Ottawa. The flume is 30.1m in length, 1.5 in width, 0.5m in height.The Flume is constructed of concrete. Water is pumped into the flume and a swing gate was installed 21.5m downstream from flume inlet separating the reservoir from the actual flume test section. Dam break waves with different characteristics were generated by the rapid opening of the gate (in a very short time (t = 0.06–0.08 s). A movable steel gate installed at the downstream end of the flume ensures that a layer of water can be maintained for various wet bed conditions (different water levels). Figures 1 and Figure 2(b) illustrate the flume in plan and side view respectively. The pipe used in the tests is a steel pipe with a 10 cm diameter, which is located at x=6 m downstream of the swing gate. Experiments were conducted with different relative gap ratios, e/D=0.3, 0.6, 0.8, *e* being distance to the flume bed and *D* (pipe diameter), different tailwater depths for wet bed condition (d=0-22cm) and with three different reservoir (impoundment) depths (h=30cm, 40cm & 50 cm) and different components of the force exerted on the pipe were measured.

2.2. Instrumentation

Figure 1, shows a schematic of the location of the instrumentation used in the tests, while Figure 2(a) & 2(b) show images of the instrumentation and its location.

2.2.1. Wave gauges

To measure the time-history of the water level at different locations, level three wave gauges (Akamina technology) were used. The wave gauge 1 was installed right upstream from the swing gate and is used to record the water level variation upstream of the gate. The recorded data can be used for the purpose of helping synchronize all othere recordings.
The other two wave gauges (2 and 3) are located at x=3.0m and x=5.6m downstream of the gate.

2.2.2. Acoustic Doppler Velocity meter (ADV)

A high-resolution acoustic Doppler velocity meter (Vectrino, SE8660) was used for velocity measurements. The ADV is able to measure water velocities along three axis using Doppler processing technology. The ADV's sampling rate was set to 200 Hz and it was located at x=5.6 m downstream of the swinging gate and placed 10 cm upstream from outer edge of the pipe. Each experimental test with a given configuration was repeated 3 times and the ADV head was vertically placed at different elevations corresponding to the level of the center of the pipe, its lower side and 5 cm away from the bottom of the flume.

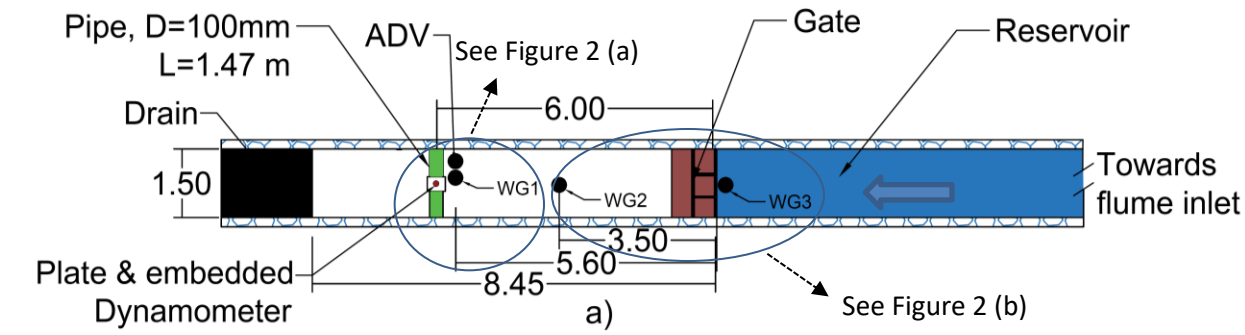

Figure 1: Flume and instrumentation. a) Plan view (unless otherwise specified, all dimensions are in m).

(a) (b)

Figure 2: a) Side view, pipe, ADV and wave gauge, b) side view - flume and gate.

2.2.3. Dynamometer

In order to record time-history of the forces exerted on the pipe due to the dam break wave, a six degrees of freedom (6DOF) dynamometer (Interface- 6A68E) was used. This dynamometer is able to simultaneously measure forces moments along the 3 axis of coordinates (*X*-*Y*-*Z*). Six full bridges provide mV/V output on 6 independent channels. The dynamometer was installed beneath the concrete flume floor by cutting the concrete, placing the device and embedding it again with concrete around as shown in Figure 3. Steel plate was placed on top in a way that the plate was leveled with the flume (Figure 2.a). The pipe is attached to the plate using two thin plates. Extra drag forces exerted because of the plates were tested and proved to be negligible. The loading exerted on the pipe was transmitted to the dynamometer through four bolts which connected the plate on which he pipe rested with the dynamometer.

2.2.4. Data acquisition system

The analog voltage signals from the instruments used in the experiments were converted to digital format and saved into data files using a QuantumX data acquisition system (MX840B, 8-channel universal amplifier & MX1601B with 16 individually configurable channels with sample rates up to 19.2 kS per channel and a bandwidth of up to 3 kHz.). All data were time-synchronized.

Figure 3: Dynamometer embedded in the flume floor

3. Experimental results and discussion

Results for drag force from testing different reservoir and tailwater depth values for different e/D values in wet and dry bed conditions, are presented below. As mentioned in Introduction section, the ratio e/D=0.3 has been shown to be the critical ratio for vortex shedding suppresion in previous studies deadling with the hydrodynamic loading on circular cylinders in constant and oscilatory flows. Results from this study demonstrated the validity of the critical e/D ratio for dam break flows over a dry bed.

3.1. Validation of the model

Multiple tests with identical initial conditions were carried out to verify the repeatability of the tests. Figure 4, represents the wave height in dry and wet bed conditions at x=3.5 m. Figures for both dry and wet bed conditions show good agreement in a way that oscillations remain the same in different tests with same release and bed conditions.

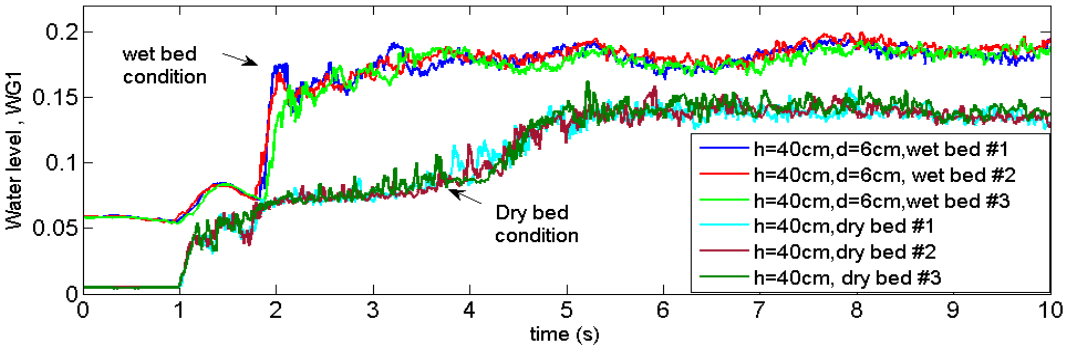

Figure 4: Repeatability of tests in dry and wet bed conditions

3.2. Evaluation of drag force for dry bed conditions and different (e/D) ratio

Analyzing the force time history in a dry case and different distance to bottom ratios, in Figure 5(b), one can observe that for e/D=0.3, the drag force behaviour is considerably different when compared to data obtained using other e/D ratios. For this particular value of e/D=0.3,two force peaks are noticed and they are defined as impulse and run up force while for values of e/D of 0.6 and 0.8, no such distinct impulse peak is observed. This phenomenon could be explained by vortex shedding suppression for such small e/D values. The vortex shedding deflects part of the fluid from upstream of the plane boundary over the top of the circular cylinder and thus reduces the flow passing through the gap (Lin et al. 2009). For values of e/D=0.6 and 0.8, the flow first passes through the gap between the pipe and the flume bed and and then reaches vertically the pipe in a very short time: hence, the presence of a rising time observed for the force to reach its maximum value.

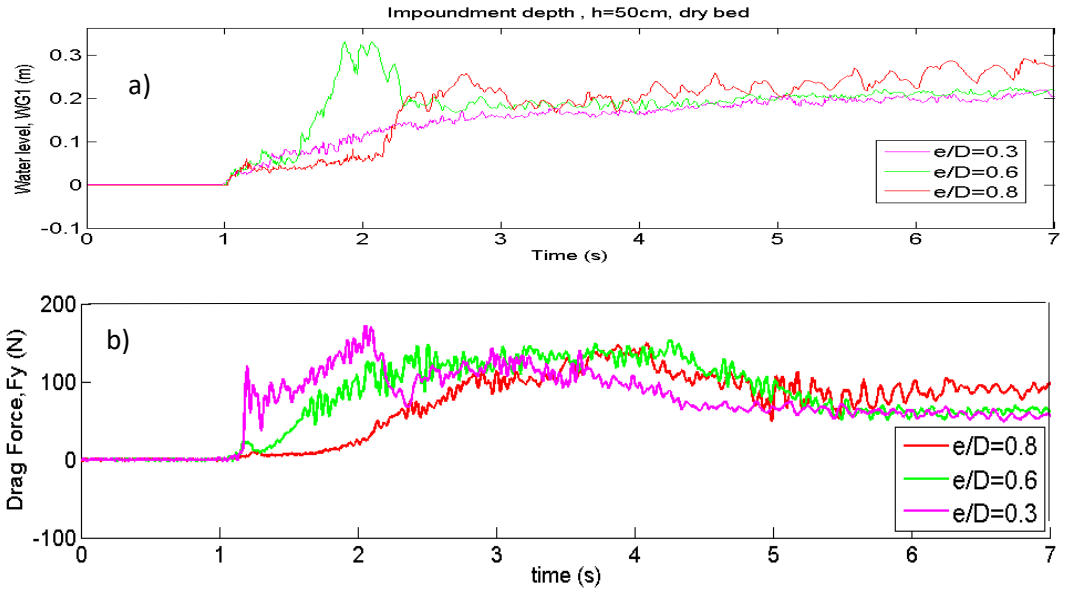

Figure 5: Time-history of the a) water level, WG1 b) drag force for dry bed condition, impoundment depth h=50cm, e/D=0.3,0.6,0.8.

3.3. Evaluation of drag force for wet bed conditions and different (e/D) ratio

Figures 6.a and 6.b illustrate hydrodynamic force components in the case of wet bed condition with *h/d=5.*0. The hydrodaynamic force time-history in wet bed condition shows a different pattern comapring to the case when using dry bed condition at the time of bore impact: the impulse force is significant comparing to the case of the force magnitude at the same instant when usign a wet bed. According to Yeh, [2007] impulse force increases due to the impact of a steeper bore front onto the object: hence the absence of a clear impulse force for the case of the dry bed condition can be attributed to the comparatively milder slope of the bore front for the dry bed condition. From Figure 5, one can reasonably conclude that drag force pattern does not change drasticaly when changing the gap ratio (e/D). Only the horizontal impulse force (Fy) decreases as the pipe submerges into the water and by placing it closer to the flume floor (decreasing the gap). The time-history of the force under similar conditions but with wet bed and with different h/d ratios, i.e, h/d=6.25, 4.16 etc, shows that impulse force is the maximum force in all these configarations. This is different from the results presented by Palermo et al. [2012] for a vertical square model in which the water reflecting from the obstacle after the first impact rejoins the incoming bore, surges up the model and causes larger forces to be exerted onto the object, a comonent that the authors identified as *run up force*. The reason behind the runup force being larger than the impulse force for vertical obstacles, is the relatively small surge depth to obstacle width ratio which causes a transient amount of added ponded water to surge against the front wall of the obstacle until it finally passes around side walls. In this study, the pipewidth is equal to flume width, therefore there is no opportunity for the water to flow past the obstacle, thus decreasing the force. Hence, the runup peak force is not recorded in this case.

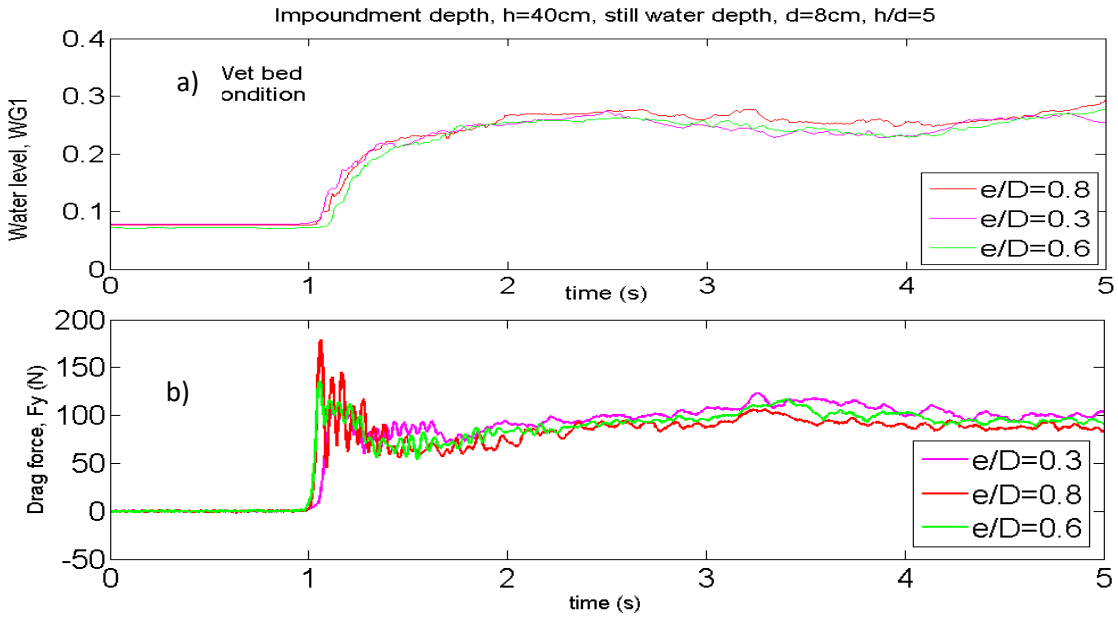

Figure 6: Time-history of the a) water level, WG1 b) drag force, for wet bed condition, h/d=5, e/D=0.3,0.6,0.8.

3.4. Drag coefficient

Results for horizontal velocity and the calculated drag coefficient for the circular cylinder impacted by the dam break wave are shown in Figure 7.a and b, respectively. In Figure 7.a colored lines show weighted average measured velocity at different elevations (z=5cm, z=8cm, z=12cm), for different relative gap ratios, i.e. e/D=0.8, e/D=0.6 and e/D=0.3.The black line shows the velocity measured in the absence of pipe. The ADV results for the first two seconds following bore impact exhibited extensive noise and were not considered in this analysis. Bore front velocity which is important for calculating the impulse or slam coefficient will be derived using image processing and analysis technics in the next step of this comprehensive experimental program.

In figure 7.b, one can be observe that the magnitude of the velocity in the absence of pipe is larger than for all cases with the pipe installed with any relative gap ratio. The average velocity decreases as the gap ratio increases from e/D=0.3 to e/D=0.8, which indicates that larger gap ratios increases momentum loss. Figure 7.b shows the time-history of the drag coefficient, *Cd*, which was calculated using the experimentally-measured drag force and the weighted depth averaged velocity U in the vicinity of pipe as in Equation [5.1]

$$[5.1] \quad C_D = \frac{1}{2}\rho U^2 / F_D$$

Where F_D is the horizontal component of the force exerted on the pipe, U is horizontal velocity and ρ is water density considered as 1000 kg/m^3.

The highest and lowest Cd values occur for the case of the pipes with e/D=0.8 and e/D=0.3, respectively, which once again, indicated more momentum loss within the case of larger gap ratios. The values of Cd derived using the velocity in the absence of pipe are lowest of all other configurations which indicates that using this velocity to drive the drag coefficient for pipeline design may result in underestimating the drag force and may hence lead to possible damage to the pipeline in the case of an extreme hydrodynamic event. Safety factors should be considered for this reason in pipe design guidelines.

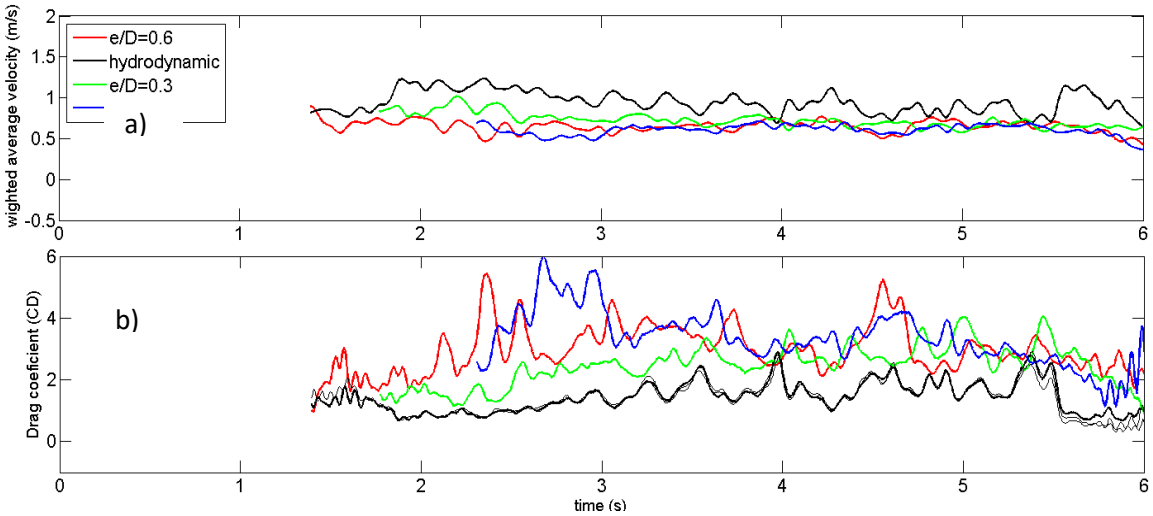

Figure 7: Time-history of: a) Horizontal velocity measured using ADV, b) Calculated drag coefficient using measured drag force and the horizontal velocity. Colored: different e/D ratios, black: pure hydrodynamic.

4. Numerical model

The 1-D shallow water equations were used to simulate the dam break flow over a flat flume and its flow pasta circular cylinder located downstream of the swinging gate. The 1-D Navier-Stockes equations consist of the conservation of mass.

$$[4.1] \quad \frac{\partial h}{\partial t} + \frac{\partial uh}{\partial x} = 0$$

$$[4.2] \quad \frac{\partial uh}{\partial t} + \frac{\partial (u^2 h + 0.5gh^2)}{\partial x} = gh(S_0 - S_f)$$

Where, *u(x,t)* is the flow velocity, *h(x,t)* is the instantaneous water depth, *S*(*x*) is the bed slope and $S_f(x,t)$ is the friction slope.

An isolated obstacle impacted by the flow, will add a new momentum source term to Eq. 4.2 as the drag increases in the vicinity of the obstacle. This extra momentum was incorporated in the momentum equation as the second term to the right side of Equation 4.3, using drag coefficient C_D.

$$[4.3] \quad \frac{\partial uh}{\partial t} + \frac{\partial (u^2 h + 0.5gh^2)}{\partial x} = gh(S_0 - S_f) + C_D u^2$$

The dam break flow in the presence of a half pipe with its major axis=0.16 and minor axis=0.1 was numerically simulated by solving the modified 1-D shallow water equations [4.1] & [4.3] using a MATLAB code developed by the authors. The results of the water surface time history obtained with the proposed numerical model were compared with the experimentally-recorded data for the case with dam break flow over a horizontal circular cylinder with diameter=0.1 and gap ratio e/D=0.6d. Reservoir depth was set to $d_0 = 40cm$.

5. Numerical results

Figure 8.a & b show results for water level from numerical model using 1D shallow water equations, at t=0 and t=10s, while, Figure 8. shows the comparison between results for water surface elevation time history derived from numerical simulation with different Cd values used in equation [4.3] and experimental results in e/D=0.6.

As can be seen in the Figure 9. results for drag coefficient from numerical and experimental study with same impoundment depth do not match perfectly. As the Cd value is increased from 0.8 to 4 the peak in water surface time history is shifted to the right and results get closer. The reason behind this difference is mainly the fact that, 1D equations are unable to simulate vertical velocities accurately. Drag coefficient is mostly dependent on the shape of the obstacle and this caused the results from simulations to be inaccurate. However, such simulations could be used for obtaining a rough estimate for a constant drag coefficient for design purposes.

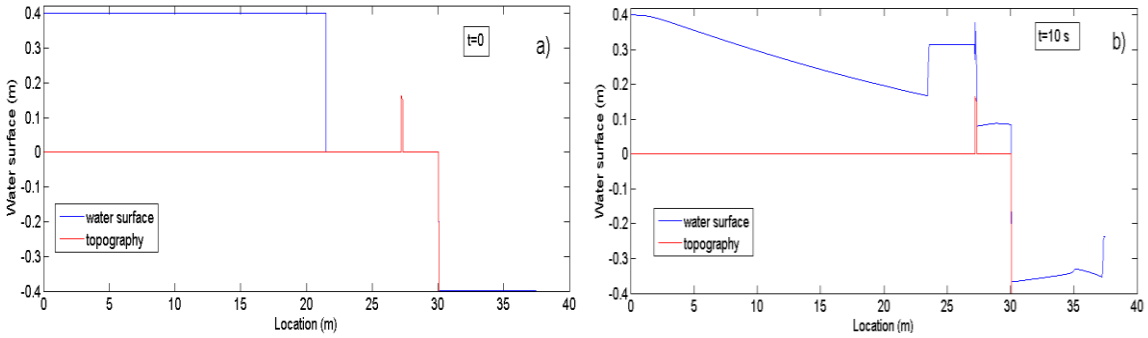

Figure 8: Results of the numerical models using the 1-D shallow water equation a) t=0, b) t=10s.

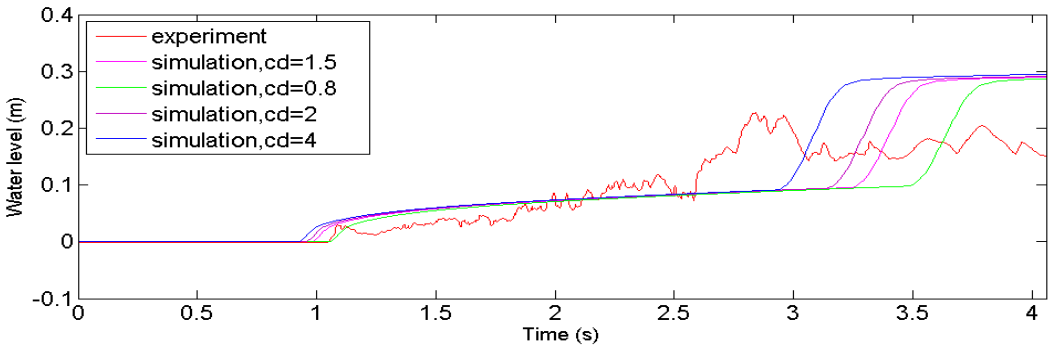

Figure 9: Comparison between experimental data and numerical time –history of the water surface of a dam break wave generated by an impoundment depth of 40 cm.

6. Conclusions

An experimental program of physical model testing was conducted to study the evolution of the hydrodynamic forces exerted on a pipe due to dam break flow which could be representative for an extreme hydrodynamic event such as tsunami-induced inundation. Force time-history was measured and analyzed for different experimental conditions with respect to changing both the tested pipe distance to bottom using gap ratio (e/D) and flow characteristics using different reservoir and both dry and wet bed conditions. Most important remarks from this study are:

- The impulse force at the time of the initial bore impact is more pronounced for the case of wet bed condition. For the case of the dry bed condition, the hydrodynamic force increases gradually until it reaches its maximum value.
- For the dry bed condition, time history for different relative gap ratios (e/D=0.3, 0.6, 0.8) was studied. Only for e/D$\leq$ 0.3, a peak force, termed impulse force at the beginning of the bore impact and later a larger peak as run up force were observed. Vortex shedding suppression at such small gap ratios causes this results to be observed. This result confirms previous finding of other

researchers for steady and oscillatory flows which confirm that e/D=0.3 is indeed a critical gap ratio for vortex shedding suppression.

- Drag force time-history for wet bed condition shows no variation, irrespective of the gap ratio.
- The drag coefficient calculated using the time-history of the velocity obtained from ADV measurements in the absence of the pipe exhibits lower magnitudes compared to the measurements when the pipe is installed. This indicates that calculations based on the latter, as suggested in many studies, may lead to underestimating the drag force for pipe design purposes.

- The 1-D shallow water equations are able to reproduce the dam break wave formation and propagation and can be used to derive the drag coefficient.

Measuring the lift force exerted onto pipelines due to dam break flows as well as calculating lift coefficient will be the focus of future studies on this topic. Image analysis technics will be used for deriving the slam coefficient at the instance of bore impact. The 3-D shallow water equations will be also employed for a more accurate numerical simulation of the problem.

References

Angrilli, F., Bergamaschi, S. and Cossalter, V., 1982. Investigation of wall induced modifications to vortex shedding from a circular cylinder. *Journal of Fluids Engineering*, *104*(4): 518-522.

Arnason, H., 2005*. Interactions Between an Incident Bore and a Free- Standing Coastal Structure, Ph.D. dissertation, University of Washington, Seattle, Washington.*

Bearman, P.W. and Zdravkovich, M.M., 1978. Flow around a circular cylinder near a plane boundary. *Journal of Fluid Mechanics*, *89*(01): 33-47.

Buresti, G. and Lanciotti, A., 1992. Mean and fluctuating forces on a circular cylinder in cross-flow near a plane surface. *Journal of Wind Engineering and Industrial Aerodynamics*, *41*(1-3): 639-650.

Chock, G. Y. 2016. Design for tsunami loads and effects in the ASCE 7-16 standard. Journal of Structural Engineering, ASCE:04016093.

Cross, R. H., 1967. Tsunami surge forces. *Journal of Waterways and Harbor Division, ASCE, 93(4): 201-231.*

FEMA. 2012. P646 Guidelines for Design of Structure for Vertical Evacuation from Tsunamis. Federal Emergency Management Agency.

Lei, C., Cheng, L. and Kavanagh, K., 1999. Re-examination of the effect of a plane boundary on force and vortex shedding of a circular cylinder. *Journal of Wind Engineering and Industrial Aerodynamics*, *80*(3): 263-286.

Lin, W.J., Lin, C., Hsieh, S.C. and Dey, S., 2009. Flow characteristics around a circular cylinder placed horizontally above a plane boundary. *Journal of engineering mechanics*, *135*(7):697-716.

Morison, J.R., Johnson, J.W. and Schaaf, S.A., 1950. The force exerted by surface waves on piles. *Journal of Petroleum Technology*, *2*(05): 149-154.

Palermo, D., Nistor, I., Al-Faesly, T. and Cornett, A., 2012. Impact of tsunami forces on structures: the university of Ottawa experience. *Fifth international tsunami symposium,Ispra, Italy,*: 3-5.

Ramsden, J.D., 1993, Tsunamis: Forces on a Vertical Wall Caused by Long Waves, Bores, and Surges on a Dry Bed, Report No. KH-R-54, W.M. Keck Laboratory, California Institute of Technology.

Stoker, J. J., 1957. Water Waves: The Mathematical Theory with Applications. *Wiley-Interscience, New York.*

Yeh, H. 2007, Design Tsunami Forces for Onshore Structures. *Journal of Disaster Research*, 2(6): 531-536

Zdravkovich, M.M., 1985. Forces on a circular cylinder near a plane wall. *Applied Ocean Research*, *7*(4): 197-201.